Sensor and Simulation Notes

Note 441

A Two-Channel Balanced-Dipole Antenna (BDA) With Reversible Antenna Pattern Operating at 50 Ohms

Everett G. Farr
Farr Research, Inc.

Carl E. Baum, William D. Prather, and Tyrone Tran
Air Force Research Laboratory / Directed Energy Directorate

December 1999

Abstract

We provide here a new design for a sensor related to the Balanced Transmission-line Wave (BTW) sensor with enhanced sensitivity. The new device is called a Balanced-Dipole Antenna (BDA), because it maintains a balance between the electric and magnetic dipoles. By exchanging the load and excitation port, this antenna can be used to look either left or right on an aircraft. The characteristics of the BDA are calculated using a Method of Moments solution to a static Poisson's equation. Design guidelines are provided to give optimal impedance match for a single-ended version of the sensor against an infinite ground plane, in order to provide a 50 Ω match at late times.

I. Introduction

A number of PxM antennas have been discussed in previous articles [1-4]. This class of antenna is normally used in place of standard B-dot or D-dot sensors, where a directional, or cardioid pattern is required. Such a device has a pattern that is proportional to $1+\cos(\theta)$ in both principal planes. The cardioid pattern is due to a balance of the electric and magnetic dipole moments. Other antennas that can be used on aircraft are discussed in [5].

The sensitivity of PxM antennas is determined by its loop area, and by its impedance match. In [2], Farr *et al* described a BTW with a small loop area, and with low sensitivity. In [3, 4], Tesche *et al* described a class of PxM antennas with larger loop area, but with impedance mismatches that also reduced the sensitivity somewhat.

In this paper we introduce a new PxM antenna that has a large loop area, and that is matched to 50 ohms impedance at late time. The new configuration is called the Balanced Dipole Antenna, or BDA. The BDA consists of a semi-cylinder against a ground plane, with connections to 50 ohm cables or loads on either end. Such a device has a much higher electric dipole moment than a cable above a ground. This tends to lower the load impedance, making it easier to provide a late-time match to 50 ohms, which is commonly used in cables.

By matching the antenna to 50 ohms, we can achieve an interesting result. If we use the BDA with a suitable switch, we can electronically switch the look direction of the antenna by 180 degrees. Thus, a BDA located on the top or bottom of an aircraft fuselage could be steered electronically to look left or right, depending on the switch position. We call this feature a reversible antenna pattern. Furthermore, if we use an array of BDAs, we can have a steerable array that can have 360 degree coverage, if time delays are included.

Previous work on loaded loops or loop monopoles has appeared in [6-10]. In [6], a combined E and B-dot sensor is described. In [7], the measurement errors in a singly-loaded B-dot sensor are described. It was found there that electric field coupling reduced the accuracy, so a doubly-loaded loop was recommended. In [8], a combined loop and electric dipole is described that provides a directive pattern. In [9], a loaded loop is described that has equal electric and magnetic field responses. In [10], a loop is considered with a distributed load impedance.

We begin by describing the new geometry of the BDA, and how it can be configured to look left or right on an aircraft. We then review the calculation technique described in [3, 4], and we describe how to extend it to the new geometry. Next, we provide general expressions for BDA performance in both transmission and reception, for arbitrary angles of incidence. Finally, we provide the equations for BDA performance when they are part of an array.

II. Geometry of the BDA

The geometry of the BDA is shown in Figure 2.1. Here we see a semi-cylindrical sheet of thin conductor above an infinite ground plane. There is a small gap between the semi-cylinder and the ground plane on either end. One of the two gaps is loaded with a resistor, and the other gap is the location of the feed connector. By making the loop broad, we lower its inductance, in a manner similar to B-dot loops [11] and the MGL sensor [12-14].

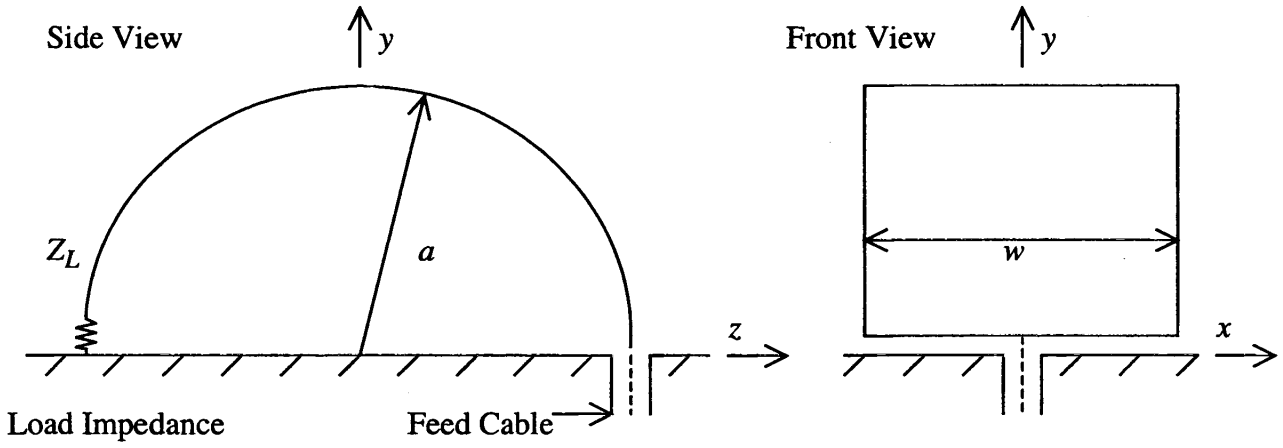

Figure 2.1 Geometry of the BDA.

Note that the impedance of the BDA is not matched at early times. Only the late-time impedance is matched to 50 ohms. So the impedance is matched only for signals with risetime lengths that are larger than the diameter of the semi-cylinder by a factor of 3 or so. We could easily achieve both an early-time and late-time match by configuring the BDA as a transmission line or BTW, as described in [2]. However, this configuration has considerably less sensitivity and area than the semi-cylindrical design. More area is available with the cable-based designs of [3, 4], however these designs are not impedance-matched at either early or late time, so there is loss due to impedance mismatch. Of all the designs considered so far, we believe the semi-cylindrical design described here provides the optimal sensitivity for a given risetime or bandwidth.

If the BDA is configured such that the required load impedance is 50 ohms, we can then replace the load with a 50 ohm cable. We can now feed the antenna from either side, sending the maximum antenna pattern either to the left or right. This configuration is shown in Figure 2.2. The antenna pattern for the configuration shown in Figure 2.2 has a maximum looking to the left ($-z$ direction), but if the antenna is fed from the right, it then has a maximum looking to the right ($+z$ direction). Thus, we say that the pattern is reversible.

A key component of the reversible pattern of the BDA is the loaded A/B switch. This is nothing more that a single-pole, double throw (SPDT) switch, with a 50 ohm load attached to the open port. Such devices are commercially available, with bandwidths up to a few gigahertz.

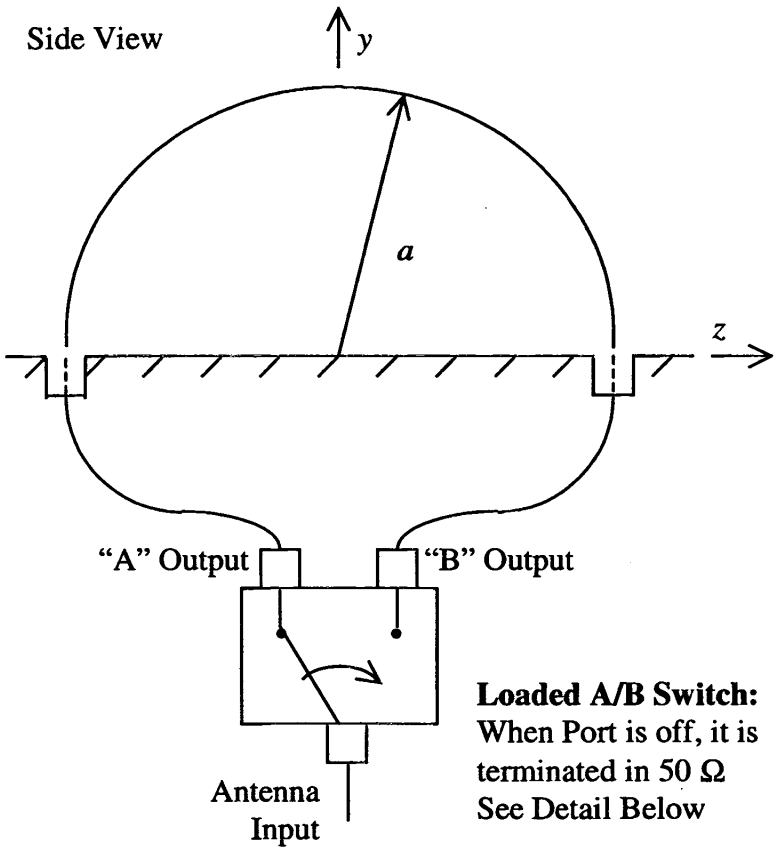

Figure 2.2. Configuration for using the BDA as a reversible antenna, which can look either left or right depending on the switch setting. With the switch set to "A", the antenna looks left.

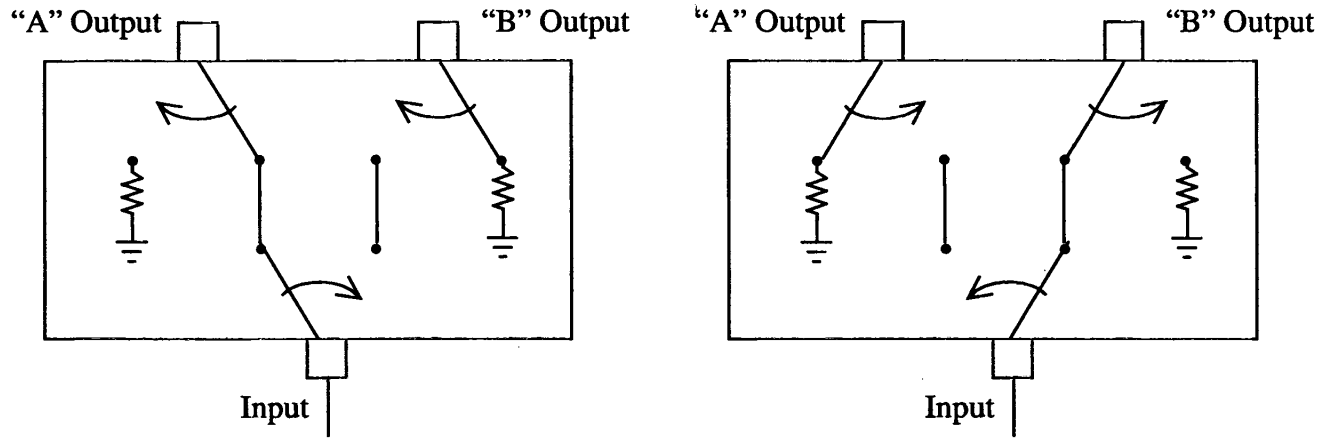

Figure 2.3. Loaded A/B switch, with switch set to "A"(left), and to "B" (right).

Note that if the BDA is used just in receive mode, then it can be used to look both left and right simultaneously. This is accomplished by removing the switch, and attaching a 50-ohm receive channel to both ports A and B. A similar idea was discussed in [5]. In this configuration, the transmit and receive antennas are different.

One might consider a few improvements to the basic design. In particular, one might taper the cylinder near the feed points on either end, in order to provide a cleaner match to the 50-ohm cable. This technique is used commonly in MGL sensors, as described in [13, 14]. The angle of the taper would provide a 50-ohm match at early time. Furthermore, at a single port, one might split the feed into two 100-ohm lines, and feed the line with two 100-ohm lines with two 100-ohm tapers. This would tend to spread out the feed point more uniformly over the gap, and this is also commonly done in MGL sensors [14]. Niether of these two improvements is included in the numerical calculations of this paper, although they may be included in a later paper.

Finally, we note that an array of reversible BDAs can be placed either on the top or bottom of an aircraft fuselage, as shown in Figure 2.4. In this manner, one can obtain a steerable array, with a narrower beam than what could be achieved with a single element. The steerability is implemented by inserting a set of time delays into each array element, either electronically or mechanically. With suitable time delays, one could achieve nearly 360 degree coverage in azimuth.

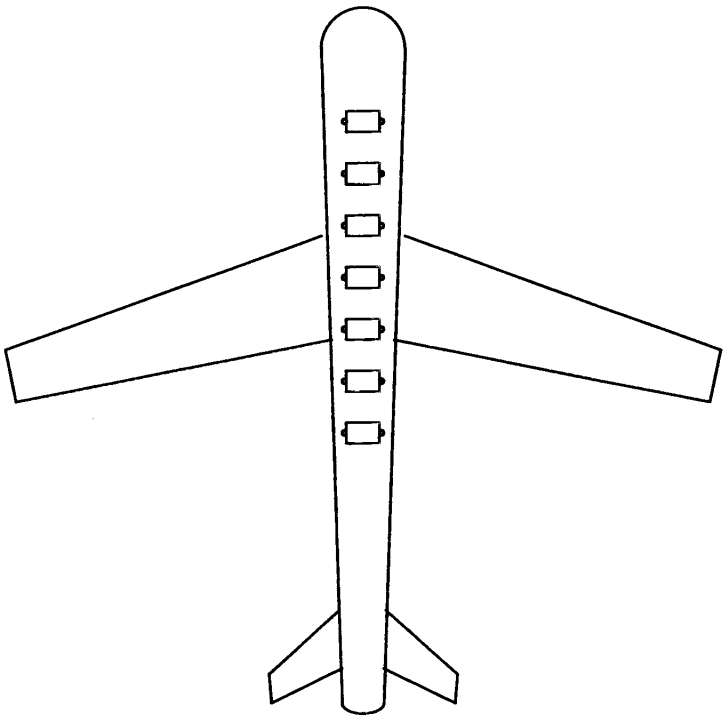

Figure 2.4. Possible arrangement of an array of reversible BDAs on the top or bottom of an fuselage, to look either left or right.

III. Theory

The calculation method used here is a straightforward extension of that used in [3, 4]. In that paper, Tesche *et al* balanced the electric and magnetic dipoles of a wire PxM antenna above a ground plane. The technique involved using a static method of moments code to calculate the electric dipole moment of a wire. Furthermore, they used the loop area to calculate the magnetic dipole moment. Finally, they balanced the electric and magnetic dipole moments by choosing the correct load resistor. Since the wires were rather thin, the load resistor was typically on the order of 500 ohms. In this paper, we replace the wire with a semi-cylindrical shell, in order to increase the electric dipole moment, and reduce the value of the resistor. When the semi-cylinder has a certain aspect ratio, the load impedance is 50 ohms, which provides a good match to cable.

There is little difference between the technique of [3, 4] and the technique of this paper. Because we are using a cylindrical shell instead of a wire, the method of moments calculation of the electric dipole moment must be modified to use rectangular plate basis functions, rather wire segments. Other features of the calculation remain the same.

We begin the analysis with the requirement that the electric and magnetic dipole moments are related by the speed of light in free space, or

$$c\,p_y = -m_x \tag{3.1}$$

where p_y and m_x are the electric and magnetic dipole moments in the x and y directions. Furthermore, magnetic dipole moment is simply the current times loop area, for both the cylinder and its image, so

$$m_x = -2AI = -2\pi a \frac{V_o}{R_L} \tag{3.2}$$

where $A = \pi a$ is the area of the semi-cylinder, I is the quasi-static current on the semi-cylinder, V_o is the quasi-static voltage on the semi-cylinder, and R_L is the load impedance. Combining the above two equations, we find the load impedance required to balance the dipole moments as

$$R_L = \frac{2\pi a V_o}{c\,p_y} \tag{3.3}$$

All that is left now is to find the electric dipole moment p_y.

The electric dipole moment is calculated by removing the load resistor and charging the semi-cylinder to V_o. A charge distribution $\sigma(\vec{r}')$ is set up on the cylinder, where $\vec{r}'$ specifies a location on the semi-cylinder. To find the charge distribution, we solve a static Poisson's equation, or

$$V_o = \frac{1}{4\pi\varepsilon_o}\left[\iint_{semi-cyl}\frac{\sigma(\vec{r}')\,dS'}{|\vec{r}-\vec{r}'|} + \iint_{\substack{semi-cyl\\image}}\frac{\sigma^*(\vec{r}')\,dS'}{|\vec{r}-\vec{r}'|}\right] \tag{3.4}$$

where $\sigma^*(\vec{r}') = -\sigma(\vec{r}')$ is the charge distribution of the image of the cylinder in the ground plane, and dS' is a unit of surface area on the semi-cylinder. To solve this efficiently, we have to take advantage of two planes of symmetry, the x-y plane and the y-z plane. Once we have found the charge distribution, $\sigma(\vec{r}')$, we can find the dipole moment simply as

$$p_y = \iint_{semi-cyl} y'\,\sigma(\vec{r}')\,dS' + \iint_{\substack{semi-cyl\\image}} y'^*\,\sigma^*(\vec{r}')\,dS' \tag{3.5}$$

where $y'^* = -y'$ is the location of the image of a charge element. This provides the final result we need to give us the electric dipole moment.

To solve the integral equation we use pulse basis functions and point matching. The details are quite similar to a problem solved by Harrington in [15], so we refer the reader to that book for additional details. The basis functions are flat rectangles, of sufficient quantity to provide a good approximation to the semi-cylinder. Approximately 50 basis functions are used to approximate the arc of the semi-cylinder. The width of the basis functions are then chosen so that the rectangular basis functions are approximately square.

The difficult portion of the solution is the integral over the singularity, where $\vec{r} = \vec{r}'$. In that case, the integral must be carried out analytically, and is done so in [15, eqn. 2-31]. For our rectangular basis functions, we assume the singular integral is the same as it would be for a square of the same area.

Next, we provide results in the section that follows.

IV. Results

We calculated the load impedance required to balance the dipole moments for a range of geometries. This impedance is a function of the ratio of cylinder width, w, to cylinder radius, a, and the results are shown in Figure 4.1. We find that when $w/a = 1.9$, the load impedance is 50 ohms. This provides a nice late-time match to a standard cable. Another point of interest might be at an impedance of 100 ohms, where we need $w/a = 0.6$. This might be useful if one has two halves of a sensor that feed into a single 50 ohm line.

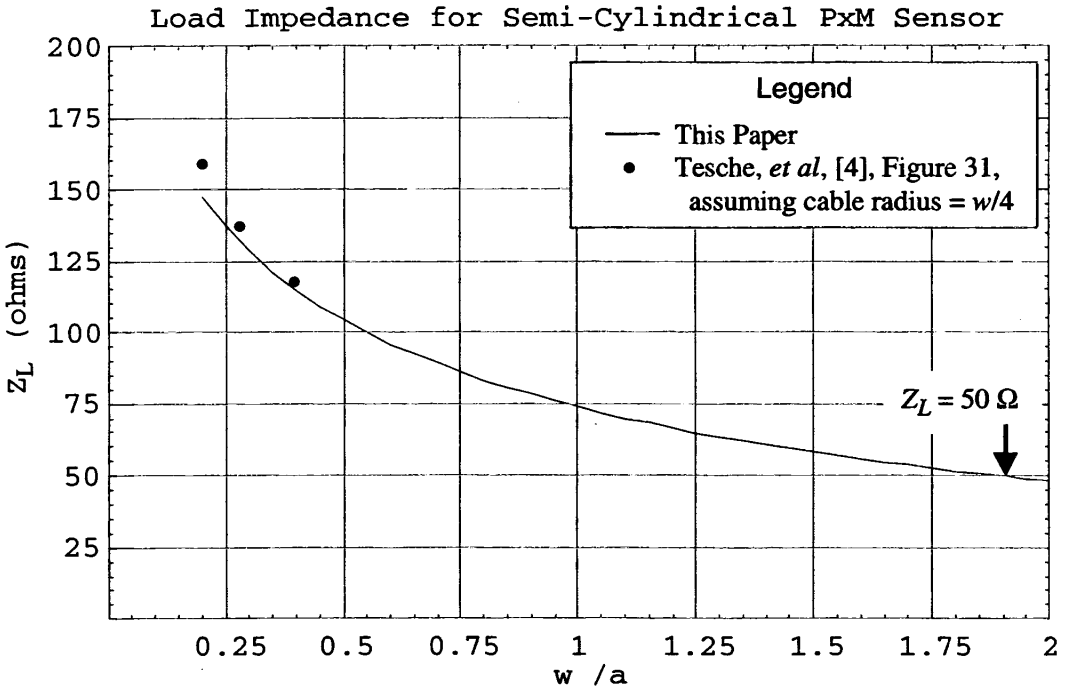

Figure 4.1. Load impedance for a semi-cylindrical P×M sensor as a function of width-to-radius ratio.

We can check our results now by comparing to the data of [4]. We are able to do so because a cable with given radius is approximately equivalent to a strip of width four times the cable radius. So we have converted a few points in [4, Figure 31] with cable radius = 1 cm to equivalent values of w/a, and we have plotted these values on Figure 4.1. From the plot we find agreement to within a few percent. Since a round cable is only approximately equivalent to a plate, this agreement seems quite reasonable.

V. Transmission and Reception with a BDA

Let us calculate now the received voltage for a BDA for arbitrary polarization and angle of incidence. Note that the BTW is a subset of a BDA, so the analysis is also valid for the BTW. The sensor is oriented as shown in Figure 5.1. After we find the receiving characteristics, we generalize the expressions to the transmission case.

We assume that the incident field is TEM and arrives from a direction $\vec{1}_r$ at the origin is described by

$$\begin{aligned} \vec{E}_{inc}(t) &= (E_\theta \vec{1}_\theta + E_\phi \vec{1}_\phi)\ f(t) \\ \vec{H}_{inc}(t) &= -\vec{1}_r \times \vec{E}_{inc}(t) \end{aligned} \tag{5.1}$$

where $f(t)$ incorporates the time dependence and all the variables are shown in Figure 1. To find the voltage received by the BDA, we need both E_y and H_x. Thus, using the standard transformation from spherical to Cartesian coordinates, we have

$$\begin{aligned} E_y(t) &= \left[E_\theta \cos(\theta)\sin(\phi) + E_\phi \cos(\phi) \right] f(t) \\ H_x(t) &= \left[H_\theta \cos(\theta)\cos(\phi) - H_\phi \sin(\phi) \right] f(t) \end{aligned} \tag{5.2}$$

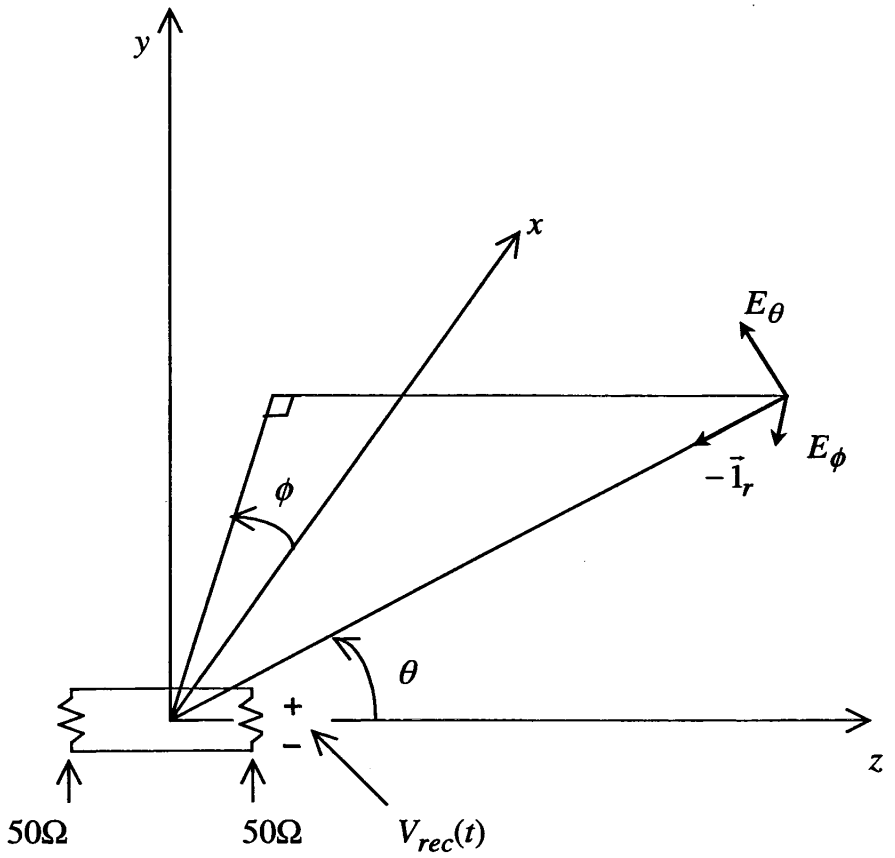

Figure 5.1. Geometry of a receiving BDA.

Furthermore, since this is a TEM plane wave,

$$H_\theta = \frac{E_\phi}{Z_o}, \quad H_\phi = -\frac{E_\theta}{Z_o} \tag{5.3}$$

where Z_o is the impedance of free space, so we have

$$H_x(t) = \frac{1}{Z_o}\left[E_\phi \cos(\theta)\cos(\phi) + E_\theta \sin(\phi)\right] f(t) \tag{5.4}$$

Having described the incident field, we now calculate the received voltage.

The received voltage is the sum of received voltages due to two effects. The first voltage is due to capacitive effect, and is due to the voltage induced across the capacitor formed by the transmission line. The second voltage is due to an inductive effect, and is due to a changing magnetic flux in the loop formed by the transmission line. The capacitive received voltage is denoted by $V_p(t)$, and the inductive received voltage is denoted by $V_m(t)$. So the total received voltage is

$$V_{rec}(t) = V_p(t) + V_m(t) \tag{5.5}$$

Using simple formulas for the voltage across capacitors and around loops, and also noting that half of the voltage is induced in each resistor (or resistive load), we find

$$V_p(t) = -\frac{1}{2}\frac{A}{c}\frac{dE_y(t)}{dt}, \quad V_m(t) = -\frac{\mu_o A}{2}\frac{dH_x(t)}{dt} \tag{5.6}$$

where μ_o is the permeability of free space, c is the speed of light in free space, and A is the area of the loop of the BDA, when looked at in along the x-axis.

While the second part of equation (5.6) is no doubt familiar as Faraday's law, the first part of equation (5.6) requires some justification. The simplest way to prove the first equation of (5.6) is that for a plane-wave incident from the along the $-z$-direction, the two voltage sources must be equal, because the dipole moments are equal. And since $E_y = c\,\mu_o\,H_x$, the two sources are indeed equal.

Another way to prove that the above equation is to calculate V_p explicitly when the BDA is a BTW composed of a 50 ohm stripline, as described in [3], with no taper sections. In this case, the stripline acts as a sensing capacitor, whose voltage is expressed as

$$V_p(t) = -\frac{Z_c}{2}I(t) = -\frac{Z_c}{2}C\frac{dV(t)}{dt} \tag{5.7}$$

where C is the capacitance of the stripline and Z_c is its characteristic impedance, 50 Ω. The stripline has a length ℓ, a width w, and a height h. If h is small compared to the risetime length of the incident field and h/w is small, then several simplifications are possible. The voltage across the plates is approximated by $V(t) \approx -h\, E_y\,(t)$ for closely spaced plates (small h). The capacitance between the two plates is $C = \varepsilon_o\, \ell\, w/h$. And the characteristic impedance across the plates is $Z_c = Z_o\, h/w$. Substituting these three relations into equation (5.7) proves the first expression in equation (5.6).

Having proven (5.6), we can now find the received voltage by combining previous results. Combining (5.5) and (5.6), we find

$$V_{rec}(t) = -\frac{1}{2}\frac{A}{c}\left[\frac{dE_y(t)}{dt} + Z_o\frac{dH_x(t)}{dt}\right] \tag{5.8}$$

Combining this with our previous expression for E_y in (5.2) and H_x in (5.4), we find

$$\boxed{V_{rec}(t) = -\frac{1}{2}\frac{A}{c}\left\{\sin(\phi)\left[1+\cos(\theta)\right]E_\theta + \cos(\phi)\left[1+\cos(\theta)\right]E_\phi\right\}\frac{df(t)}{dt}} \tag{5.9}$$

This is our final result for a single BDA element.

As a check, we can consider what happens in the two principal planes of the sensor, with dominant polarization. In the E-plane, $\phi = 90^o$, and $E_\phi = 0$. Substituting into (5.9), we find

$$V_{rec}(t) = -\frac{1}{2}\frac{A}{c}\left[1+\cos(\theta)\right]E_\theta\,\frac{df(t)}{dt} \tag{5.10}$$

This is the classic cardioid pattern, 1+cos(θ), we expect to see. In the H-plane, we have $\phi = 0^o$ and $E_\theta = 0$. Substituting this into equation (5.9) we find

$$V_{rec}(t) = -\frac{1}{2}\frac{A}{c}\left[1+\cos(\theta)\right]E_\phi\,\frac{df(t)}{dt} \tag{5.11}$$

Once again, we find the cardioid pattern that we expect, so our general result in (5.9) is consistent with our expectations.

To determine the performance of the BDA in transmission, it is simplest to recast equation (5.9) into the form of our normalized impulse response, as described in [16]. We do this so we can easily handle the case of transmission, in addition to the case of reception we have already addressed. Thus, by rearranging equation (5.9) we have

$$\frac{V_{rec}(t)}{\sqrt{Z_{cable}}} = \vec{h}_N(t) \stackrel{\circ}{:} \frac{\vec{E}_{inc}(t)}{\sqrt{Z_o}} \tag{5.12}$$

where "$\stackrel{\circ}{:}$" indicates a dot product convolution. Furthermore,

$$\begin{aligned} \vec{h}_N(t) &= \begin{bmatrix} h_{N\theta}(t) \\ h_{N\phi}(t) \end{bmatrix} = -\frac{A}{2c}\frac{\sqrt{Z_o}}{\sqrt{Z_{cable}}}\left[1+\cos(\theta)\right]\begin{bmatrix} \sin(\phi) \\ \cos(\phi) \end{bmatrix}\delta'(t) \\ \vec{E}_{inc}(t) &= \begin{bmatrix} E_{\theta\,inc}(t) \\ E_{\phi\,inc}(t) \end{bmatrix} \end{aligned} \tag{5.13}$$

where $\delta'(t)$ is the derivative of the Dirac delta function, and Z_{cable} = 50 Ω. Since we have the receive equations in the standard form, we can now simply express the transmission equations as

$$\frac{\vec{E}_{rad}(t)}{\sqrt{Z_o}} = \frac{1}{\sqrt{Z_o}}\begin{bmatrix} E_{rad\,\theta}(t) \\ E_{rad\,\phi}(t) \end{bmatrix} = \frac{1}{2\pi r c}\vec{h}_N(t) \circ \frac{1}{\sqrt{Z_{cable}}}\frac{dV_{src}(t)}{dt} \tag{5.14}$$

This completes the general description of the transmitted and received field from a single BDA.

VI. BDAs as Elements of Arrays

Let us now consider the expression if the sensor is displaced by a small amount from the origin. This will be useful if the BDA is used as part of an array.

We assume that the angle to the far field is unchanged for a sensor with only a small displacement from the origin. Thus, the sensor is located at $\vec{r}'$, and the received voltage is the same as it would be for a sensor located at the origin, with the exception of a time delay. So the received voltage is adjusted to

$$V_{rec}(t,\vec{r}') = V_{rec}(t - \vec{r}' \bullet \vec{1}_r / c,\ \vec{r}' = \vec{0}) \tag{6.1}$$

This is expressed more simply as

$$V_{rec}(t,\vec{r}') = V_{rec}(t - (r'/c)\cos(\theta_i),\ \vec{r}' = \vec{0}) \tag{6.2}$$

where θ_i is the angle between $-\vec{1}_r$ and $\vec{1}_{r'}$. This rather simple result will be useful if we build an array of BDAs. In that case, there will be several locations of BDAs denoted by $\vec{r}_i'$, and the total received voltage will be the sum of the individual responses, or

$$\begin{aligned} V_{rec}(t,\vec{r}') &= \sum_i V_{rec}(t - \vec{r}_i' \bullet \vec{1}_r / c) \\ &= \sum_i V_{rec}(t - (r'/c)\cos(\theta_i)) \end{aligned} \tag{6.3}$$

This completes the analysis required to calculate the response of an array of BDAs.

V. Conclusions

We have defined a new antenna geometry, the BDA, that is related to the BTW, and that has improved sensitivity over previous designs, for a given bandwidth. The electric dipole moment of the proposed configuration was calculated using a static Method of Moments solution to Poisson's equation. The aspect ratio to obtain a 50 ohm match is w/a=1.9.

Acknowledgement

We wish to thank the Air Force Research Laboratory, Directed Energy Directorate, for funding this work.

References

1. J. S. Yu, C-L James Chen, and C. E. Baum, Multipole Radiations: Formulation and Evaluation for Small EMP Simulators, Sensor and Simulation Note 243, July 1978.

2. E. G. Farr and J. Hofstra, An Incident Field Sensor for EMP Measurements, IEEE Trans. Electromag. Compatibility, May 1991, pp. 105-113. Also published as Sensor and Simulation Note 319, July 1989

3. F. M. Tesche, The PxM Antenna and Applications to Radiated Field Testing of Electrical Systems, Part 1, Theory and Numerical Simulations, Sensor and Simulation Note 407, July 1997

4. F. M. Tesche, T. Karlsson, and S. Garmland, The PxM Antenna and Applications to Radiated Field Testing of Electrical Systems, Part 2, Experimental Considerations, Sensor and Simulation Note 409, July 1997.

5. C. E. Baum, Antennas on Airplanes, Sensor and Simulation Note 435, March 1999.

6. R. E. Partridge, Combined E and B-dot Sensor, Sensor and Simulation Note 3, February 1964.

7. H. Whiteside and R. W. P. King, The Loop Antenna as a Probe, *IEEE Trans. Antennas and Propagation*, May 1964, pp. 291-297.

8. W. C. Wong, Signal and Noise Analysis of a Loop-Monopole Active Antenna, *IEEE Trans. Antennas and Propagation*, July 1974, pp. 574-580.

9. M. Kanda, An Electromagnetic Near-Field Sensor for Simultaneous Electric and Magnetic-Field Measurements, *IEEE Trans. Electromagnetic Compatibility*, Vol. EMC-26, August 1984, pp. 102-110.

10. K. P. Esselle and S. S. Stuchly, Resistively Loaded Loop as a Pulse-Receiving Antenna, *IEEE Trans. Antennas Propagation*, Vol. 38, No. 7, July 1990, pp. 1123-1126.

11. C. E. Baum, Maximizing Frequency Response of a B-dot Loop, Sensor and Simulation Note 8, December 1964.

12. C. E. Baum, The Multi-Gap Cylindrical Loop in Non-Conducting Media, Sensor and Simulation Note 41, May 1967

13. C. E. Baum, A Conical-Transmission-Line Gap for a Cylindrical Loop, Sensor and Simulation Note 42, May 1967,

14. C. E. Baum, *et al*, Sensors for Electromagnetic Pulse Measurements Both Inside and Away from Nuclear Source Regions, *IEEE Trans. Electromagnetic Compatibility*, Vol. EMC-20, No. 1, February 1978, pp. 22-35.

15. R. F. Harrington, *Field Computation by Moment Methods*, Krieger Publishing Co., 1982, pp. 24-27.

16. E. G. Farr and C. E. Baum, Time Domain Characterization of Antennas with TEM Feeds, Sensor and Simulation Note 426, October 1998.